

Figure 2 as the mole fraction of guest residue,  $f_X$ , versus  $T_b$ . Compositions with values of  $T_b$  below 0 °C cannot be studied because of inability to achieve the dissolved state below the freezing point of water.

From this data the relative hydrophobicities are seen to be Trp > Tyr > Phe > Leu  $\approx$  Ile  $\approx$  Met > Val > Ala > Gly. While the accuracy with which the experimental heat ( $\Delta H$ ) of the transition can be determined is less than that of the temperature, a similar scale is obtained from the difference in heats due to the substitution, i.e.,  $\delta\Delta H(X) = \Delta H(\text{VPGXG}) - \Delta H(\text{VPGGG})$  with extrapolation to  $f_X = 1$ . The results of the  $\delta\Delta H$  in kilocalories/mole are W (6.2) > F (5.6) > Y (4.6) > L (3.9) > I (3.6) > V (2.0) > M (1.8) > A (0.4) > G (0.0). Clearly, Trp comes out to be the most hydrophobic in this functional scale, and interestingly there is an interchange between the Tyr and Phe order when temperatures and heats of the transition are compared. It may ultimately be more appropriate to use an entropy scale, i.e.,  $\delta(\Delta H/T)$ . From the practical side, when the temperature scale is used, it becomes possible to choose a combination of residues that gives any desired value for  $T_b$  from  $\sim 0$  °C to about 60 °C. This sets the stage for the proper consideration of polar groups including the demonstration that  $\text{COO}^-$  is very much more polar than  $\text{COOH}$ <sup>12,25,26</sup> and allows that the temperature and heat of the transition may be used to determine the effects of other perturbations, such as NaCl and other salts, urea, guanidine hydrochloride, ethylene glycol and other alcohols, dimethyl sulfoxide, etc., on the expression of hydrophobicity.

**Acknowledgment.** This work was supported in part by the Department of the Navy, Office of Naval Research Contract N00014-89-J-1970. We also thank Bioelastics Research, Ltd., for the gift of poly[0.75(VPGVG),0.25(VPGFG)], which was prepared with the support of ONR Contract N00014-89-C-0282.

(25) Urry, D. W.; Luan, C.-H.; Harris, R. D.; Prasad, K. U. *Polym. Prepr. (Am. Chem. Soc., Div. Polym. Chem.)* **1990**, 31(1), 188-189.

(26) The temperature of the inverse temperature transition of poly[0.8-(VPGCG),0.2(VPGEG)] where E = Glu is raised by 45 °C from near 25 °C to near 70 °C in phosphate-buffered saline when the pH is raised from 2 to 7, i.e., on conversion of four  $\text{COOH}$  moieties to  $\text{COO}^-$  per 100 residues of polypentapeptide<sup>21</sup> and the heat of the transitions is reduced to less than one-fourth.<sup>25</sup>

## 2D NMR Assignment of Hyperfine-Shifted Resonances in Strongly Paramagnetic Metalloproteins: Resting-State Horseradish Peroxidase

Jeffrey S. de Ropp<sup>†</sup> and Gerd N. La Mar<sup>\*‡</sup>

*NMR Facility and Department of Chemistry  
University of California, Davis, California 95616*

*Received February 4, 1991*

Two-dimensional (2D)<sup>1</sup> NMR of small diamagnetic biomolecules is now routinely used to both assign <sup>1</sup>H resonances and determine structure. To date, these 2D methods have found much less application to paramagnetic metalloproteins in the belief that the rapid paramagnetic-induced relaxation would render cross peaks undetectable. For bond correlation or COSY data, the broad lines (short  $T_2$ 's) result in both rapid decay of coherence and extensive cancellation of antiphase cross peaks,<sup>2,3</sup> while the short  $T_1$ 's severely short-circuit the buildup of nuclear Overhauser effect or NOESY cross peaks.<sup>3,4</sup> Numerous paramagnetic me-

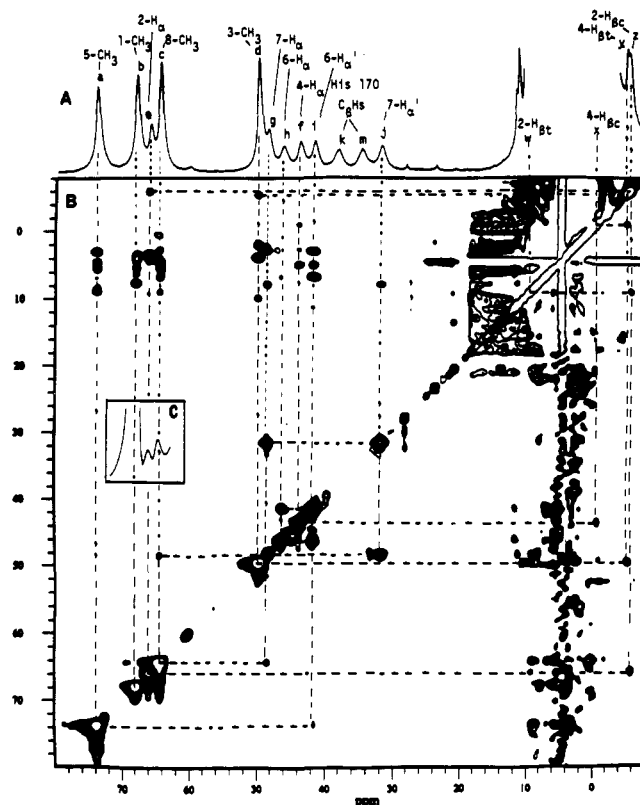


Figure 1. (A) <sup>1</sup>H NMR (300 MHz) reference trace for 3 mM HRP in a 5-mm tube in <sup>2</sup>H<sub>2</sub>O, pH 7.0 at 55 °C, with peaks labeled a-m and w-z as well as with previous assignments.<sup>10,11</sup> (B) NOESY map collected with 10-ms mixing time, with labeled cross peaks. The inset (C) gives a slice in the  $f_1$  direction through the 1-CH<sub>3</sub> on the diagonal which yields a weak cross peak to 8-CH<sub>3</sub>.

talloproteins yield remarkably well resolved <sup>1</sup>H NMR spectra,<sup>5,6</sup> for which the extraction of the significant information content of the hyperfine shifts has been thwarted by the lack of an effective assignment methodology. We have shown recently that the 1D NOE is surprisingly effective in obtaining crucial but limited assignments in both weakly<sup>7,8</sup> and strongly paramagnetic proteins.<sup>9-11</sup> The vast improvement of the information content of 2D relative to 1D NMR of small, weakly paramagnetic, low-spin ferric hemoproteins with narrow lines has been demonstrated.<sup>12,13</sup> We have shown<sup>14</sup> recently that, while paramagnetism will always diminish NOEs relative to a diamagnetic system, the paramagnetic influence is increasingly "suppressed" as the size of the protein increases. Because of the large number of paramagnetic metalloproteins that would benefit from the demonstration of effective 2D methodology, we investigate here the utility of NOESY and COSY on a moderately sized enzyme (42-kDa horseradish per-

(4) Neuhaus, D.; Williamson, M. *The Nuclear Overhauser Effect in Structural and Conformational Analysis*; VCH Publishers: New York, 1989.

(5) Satterlee, J. D. *Annu. Rep. NMR Spectrosc.* **1986**, 17, 79.

(6) Bertini, I.; Luchinat, C. *NMR of Paramagnetic Molecules in Biological Systems*; Benjamin/Cummings Publishing Co.: Menlo Park, CA, 1986.

(7) Thanabal, V.; de Ropp, J. S.; La Mar, G. N. *J. Am. Chem. Soc.* **1987**, 109, 265.

(8) Dugad, L. B.; La Mar, G. N.; Banci, L.; Bertini, I. *Biochemistry* **1990**, 29, 2263.

(9) Unger, S. W.; Lecomte, J. T. J.; La Mar, G. N. *J. Magn. Reson.* **1985**, 64, 521.

(10) Thanabal, V.; de Ropp, J. S.; La Mar, G. N. *J. Am. Chem. Soc.* **1986**, 108, 4244.

(11) Thanabal, V.; La Mar, G. N.; de Ropp, J. S. *Biochemistry* **1988**, 27, 5400.

(12) McLachlan, S. J.; La Mar, G. N.; Lee, K.-B. *Biochim. Biophys. Acta* **1988**, 957, 430.

(13) Emerson, S. D.; La Mar, G. N. *Biochemistry* **1990**, 29, 1545.

(14) Dugad, L. B.; La Mar, G. N.; Unger, S. W. *J. Am. Chem. Soc.* **1990**, 112, 1386.

(15) La Mar, G. N. In *Biological Applications of Magnetic Resonance*; Shulman, R. G., Ed.; Academic Press: New York, 1979; p 305.

<sup>†</sup>NMR Facility.

<sup>‡</sup>Department of Chemistry.

(1) Wüthrich, K. *NMR of Proteins and Nucleic Acids*; Wiley & Sons: New York, 1986.

(2) Bax, A. *Two Dimensional Nuclear Magnetic Resonance in Liquids*; D. Reidel Publishing Co.: Dordrecht, Holland, 1982.

(3) Ernst, R. R.; Bodenhausen, G.; Wokaun, A. *Principles of Nuclear Magnetic Resonance in One and Two Dimensions*; Clarendon Press: Oxford, England, 1987.

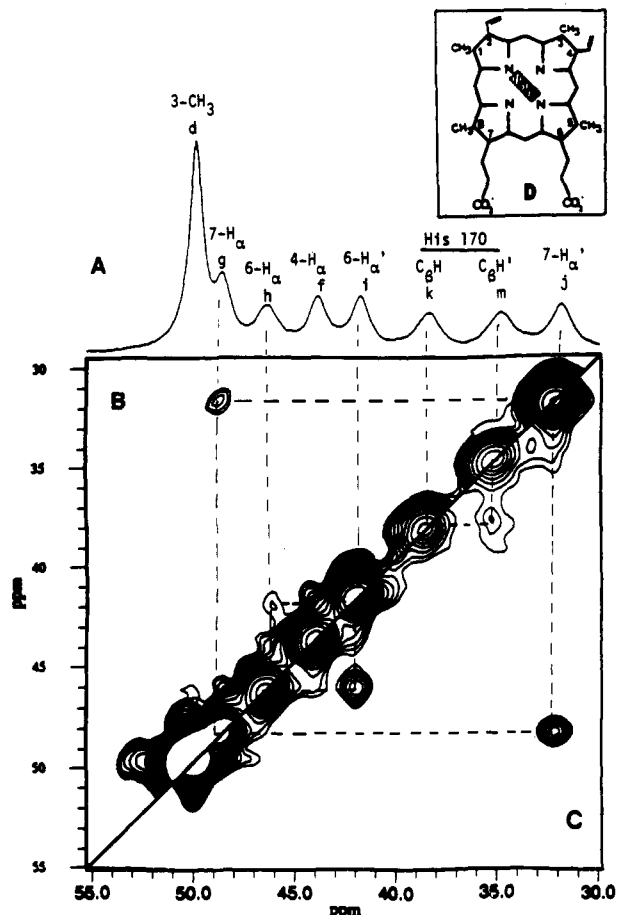


**Figure 2.** (A) Portion (55–30 ppm) of the 300-MHz  $^1\text{H}$  NMR reference trace for 3 mM HRP in a 5-mm tube in  $^2\text{H}_2\text{O}$ , pH 7.0 at 55  $^\circ\text{C}$ ; split diagonal portions of the (B) magnitude COSY map revealing the only detectable resolved cross peaks, those between the geminal protons of the  $\alpha$ -methylene groups of the two propionates; and (C) NOESY map collected with a mixing time of 3 ms that exhibits the His 170  $\text{C}_\beta\text{H}$ 's cross peak. (D) Structure and labeling of the heme group.

oxidase,<sup>16</sup> HRP) in the "worst-case scenario", high-spin iron(III) state,<sup>10,11,15</sup> with large spectral dispersion (to 100 ppm), broad lines (to 500 Hz), and short  $T_1$ 's (to 2 ms) typical of numerous strongly paramagnetic metalloenzymes. Previous labeling<sup>17</sup> and 1D NOE<sup>10,11</sup> assignments allow a critical test of the efficacy of the 2D experiments.

The 300-MHz  $^1\text{H}$  NMR trace of HRP in  $^2\text{H}_2\text{O}$  at 55  $^\circ\text{C}$  is reproduced in Figure 1A. The heme methyls, a–d (line width  $250 \pm 50$  Hz), and single protons e–j (line width  $400 \pm 50$  Hz), k, m (line width  $500 \pm 50$  Hz), and y, z (line width  $100 \pm 20$  Hz) are resolved from the intense diamagnetic envelope; previous assignments for these resonances are also given.<sup>10,11,17</sup> The NOESY map<sup>18</sup> collected at 55  $^\circ\text{C}$  with a 10-ms mixing time, optimized for detecting intraheme cross peaks,<sup>19</sup> is illustrated in Figure 1B. The most intense cross peaks in Figure 1B, also seen strongly for a shorter mixing time of 3 ms (Figure 2C), arise from

single-proton peaks g, j and h, i and reflect the strong cross relaxation of geminal protons of the propionate  $\alpha$ - $\text{CH}_2$ 's. The geminal nature of these proton pairs is confirmed by the only magnitude COSY<sup>20</sup> cross peaks observed in Figure 2B (see below). The weak cross peaks from the methylenes in Figure 1B identify the respective adjacent methyls a, c at the 5,8-positions. Vinyl groups are recognized by the moderate-intensity cross peaks between the low-field single-proton  $\text{H}_\alpha$  peaks (e, f) and the upfield  $\text{H}_{\beta\text{c}}$ 's (e, z for one vinyl, f, x for the other). The strong cross peaks from the upfield vinyl  $\text{H}_{\beta\text{c}}$ 's identify the respective  $\text{H}_{\beta\text{t}}$ 's (sets e, z, w and f, y, x), and the cross peak from d to y correlates the 4-vinyl group (f, y, x) to the adjacent 3- $\text{CH}_3$ . A weak cross peak (better seen in a slice, inset C) reveals the proximity of two methyls, 1- $\text{CH}_3$  and 8- $\text{CH}_3$ .<sup>21</sup> This leads to the complete pyrrole substituent assignment as indicated by the labeling on Figure 1A; meso H's exhibit line widths<sup>22</sup>  $> 1.5$  kHz and are not detected in the  $^1\text{H}$  NMR trace.

The complete assignments for the heme derived herein solely from two 2D experiments are the same as those previously determined by interpreting multiple 1D NOEs based on isotope labeling<sup>10,11,17</sup> and locate additionally the previously unidentified vinyl 4- $\text{H}_{\beta\text{c}}$  and 2- $\text{H}_{\beta\text{t}}$  peaks. Cross peaks between 3- $\text{CH}_3$  and 4- $\text{H}_{\beta\text{t}}$  establish a cis orientation for the 4-vinyl, while the complete absence of such a peak between 1- $\text{CH}_3$  and 2- $\text{H}_{\beta\text{t}}$  argues for a trans orientation of the 2-vinyl group (inset D to Figure 2), as proposed previously.<sup>10</sup> The cross peak between the two known<sup>23</sup> His 170  $\text{C}_\beta\text{H}$ 's (line widths  $\sim 500$  Hz,  $T_1$ 's  $\sim 2$  ms) is not detected in the 10 ms mixing time NOESY map in Figure 1B. However, at a 3-ms mixing time optimized for the most rapidly relaxing lines,<sup>19</sup> we observe not only the expected 6- $\alpha$ - $\text{CH}_2$  and 7- $\alpha$ - $\text{CH}_2$  geminal cross peaks but also the cross peak for the His  $\text{C}_\beta\text{H}$ 's (Figure 2C). A magnitude COSY<sup>22,24</sup> map, collected at 23  $\text{s}^{-1}$  with the optimal acquisition time of  $2T_2$  and pseudo-echo apodization, yielded detectable resolved cross peaks only among two pairs of resonances within the 6- $\alpha$ - $\text{CH}_2$  and within the 7- $\alpha$ - $\text{CH}_2$ , as shown in Figure 2B. Cross peaks among the protons of either vinyl group were not observed.

The data in Figures 1B and 2C clearly demonstrate that the NOESY experiment is remarkably effective in detecting spatial proximity even among extraordinarily efficiently relaxed protons. While the intensities of the cross peaks for hyperfine-shifted and relaxed lines are significantly diminished relative to those in an isostructural diamagnetic system,<sup>14</sup> effective sensitivity is readily achieved in a reasonable time because of the vastly increased repetition rates of the pulse sequence allowed by the short  $T_1$ 's. The NOESY map in Figure 1B provides all of the information needed for the assignment of the heme substituents in the absence of isotope labeling and, hence, opens up an assignment strategy for high-spin ferric hemoproteins whose hemes are not reversibly extractable.<sup>25</sup> The COSY map, on the other hand, provides much less comprehensive data, although the coherence between the propionate geminal protons is detected weakly in spite of  $\sim 400$ -Hz line widths and only  $\sim 14$ -Hz coupling. Thus NOESY spectra should find broad application for other paramagnetic metalloproteins.<sup>5,6,8,10–13,26–28</sup> *Because of the increase in cross relaxation*

(20) MCOSEY spectra were collected by using 256  $t_1$  blocks of 4480 scans each over a 60-kHz band width using 1024  $t_2$  points. The repetition rate of the pulse sequence was 23  $\text{s}^{-1}$ ; the total experiment time was 14 h. Data were processed in each dimension with 0 $^\circ$ -shifted sine-bell-squared apodization over 256 points (4 ms in both  $t_1$  and  $t_2$ ), zero-filled to  $1024 t_1 \times 1024 t_2$  points, and symmetrized.

(21) La Mar, G. N.; Emerson, S. D.; Lecomte, J. T. J.; Pande, U.; Smith, K. M.; Craig, G. W.; Kehres, L. A. *J. Am. Chem. Soc.* **1986**, *108*, 5568.  
(22) La Mar, G. N.; Thanabal, V.; Johnson, R. D.; Smith, K. M.; Parish, D. W. *J. Biol. Chem.* **1989**, *264*, 5428.

(23) Thanabal, V.; de Ropp, J. S.; La Mar, G. N. *J. Am. Chem. Soc.* **1987**, *109*, 7516.

(24) Yu, L. P.; La Mar, G. N.; Rajarathnam, K. *J. Am. Chem. Soc.* **1990**, *112*, 9527.

(25) La Mar, G. N.; Jackson, J. T.; Dugad, L. B.; Cusanovich, M. A.; Bartsch, R. G. *J. Biol. Chem.* **1990**, *265*, 16173.

(26) Maroney, M. J.; Kuntz, J. M., Jr.; Nocek, J. M.; Pearce, L. L.; Que, L., Jr. *J. Am. Chem. Soc.* **1986**, *108*, 6871.

(27) Scharrow, R. C.; Pyrz, J. W.; Que, L., Jr. *J. Am. Chem. Soc.* **1990**, *112*, 657.

(16) Dunford, H. B. *Adv. Inorg. Biochem.* **1982**, *4*, 41.

(17) La Mar, G. N.; de Ropp, J. S.; Smith, K. M.; Langry, K. C. *J. Biol. Chem.* **1980**, *255*, 6646.

(18) NOESY spectra were collected on a GE  $\Omega$ -300 NMR spectrometer in the phase-sensitive hypercomplex mode by using 512  $t_1$  blocks of 1280 scans each over a 60-kHz band width using 1024 complex  $t_2$  points; the total experiment time was 16 h. The mixing time was either 10 ms (Figure 1B) or 3 ms (Figure 2C); the repetition rate of the pulse sequence was 11  $\text{s}^{-1}$ . The residual solvent signal was irradiated during the relaxation delay. Data were processed in each dimension with 60 $^\circ$ -shifted sine-bell-squared apodization over 256 points (i.e., 4 ms  $t_1$ ,  $t_2$  acquisition time), zero-filled to  $1024 t_1 \times 1024 t_2$  points prior to Fourier transformation, phase corrected, and base-line straightened.

(19) The maximum intensity of a NOESY cross peak occurs for a mixing time approximately equal to the shorter  $T_1$  of the dipolar coupled protons.<sup>4</sup>

with size, the NOESY maps can be expected to be particularly informative for the larger paramagnetic metalloproteins, such as hemerythrins,<sup>26</sup> uteroferrins,<sup>27</sup> and various superoxide dismutase complexes.<sup>28</sup>

**Acknowledgment.** This research was supported by a grant from the National Institutes of Health, GM 26226. The GE  $\Omega$ -300 NMR spectrometer was purchased in part with funds provided by a grant from the National Science Foundation, DIR-90-16484.

(28) Banci, L.; Bencini, A.; Bertini, I.; Luchinat, C.; Piccioli, M. *Inorg. Chem.* 1990, 29, 4867 and references therein.

## Slow Conformational Dynamics at the Metal Coordination Site of a Zinc Finger

G. Marius Clore,\* James G. Omichinski, and Angela M. Gronenborn\*

Laboratory of Chemical Physics, Building 2  
National Institute of Diabetes and Digestive and  
Kidney Diseases, National Institutes of Health  
Bethesda, Maryland 20892

Received January 15, 1991

We recently described the determination of the high-resolution three-dimensional structure of a synthetic 30-residue classical Cys<sub>2</sub>His<sub>2</sub> zinc finger domain of the human enhancer binding protein in solution by NMR.<sup>1</sup> This communication extends this work to include an investigation of dynamical properties and presents direct evidence for slow conformational exchange between several species involving the histidine side chains coordinated to the zinc atom.

Figure 1 shows homonuclear Hartmann-Hahn (HOHAHA)<sup>2</sup> and nuclear Overhauser enhancement (NOESY)<sup>3</sup> spectra comprising the region of the C<sup>1</sup>H resonances of the histidine residues of 4.8 mM peptide in the presence of a molar excess of ZnCl<sub>2</sub> at pH 5.8 and 6 °C. Of the three histidine residues present in this zinc finger, the two that are liganded to zinc, His-21 and His-27, exhibit three sets of resonances, one at 7.33 and 7.75 ppm, respectively, corresponding to a major form (A), and two sets ~0.25 ppm to lower field corresponding to two minor forms (B and C). Cross peaks between these sets of resonances (labeled C,A and B,A) are seen in both the NOESY and HOHAHA spectra. As the sign of these cross peaks in the spin-locked HOHAHA spectrum is the same as that of the diagonal, and as these minor resonances do not correspond to the C<sup>2</sup>H protons of histidine, they must arise through chemical exchange.<sup>4</sup> A similar set of exchange cross peaks is also seen for the C<sup>2</sup>H proton of His-27 where the chemical shifts of the two minor forms are degenerate and ~0.39 ppm downfield of that observed for the major species. No exchange peaks were observed for the C<sup>2</sup>H proton of His-21. In addition, a number of other resonances of residues in close spatial proximity to the histidine residues also appear to exhibit exchange cross peaks, but as the chemical shift differences are smaller and they occur in crowded regions of the spectrum, they are difficult to assign

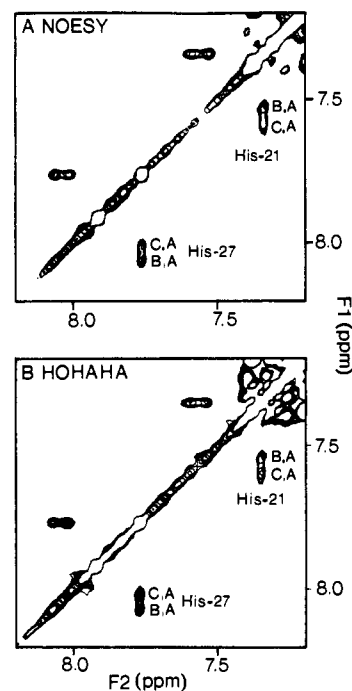


Figure 1. Histidine C<sup>1</sup>H region of the (A) 150-ms NOESY and (B) 36-ms HOHAHA spectra of the human enhancer zinc finger domain. The spin-lock field in the HOHAHA spectrum was generated by a WALTZ-17 mixing sequence<sup>2</sup> with a radio frequency field strength of ~8 kHz. Experimental conditions: 4.8 mM peptide, 50 mM ZnCl<sub>2</sub>, pH 5.8, 6 °C. (Note that identical results are obtained with a 1:1 ratio of peptide to zinc.)

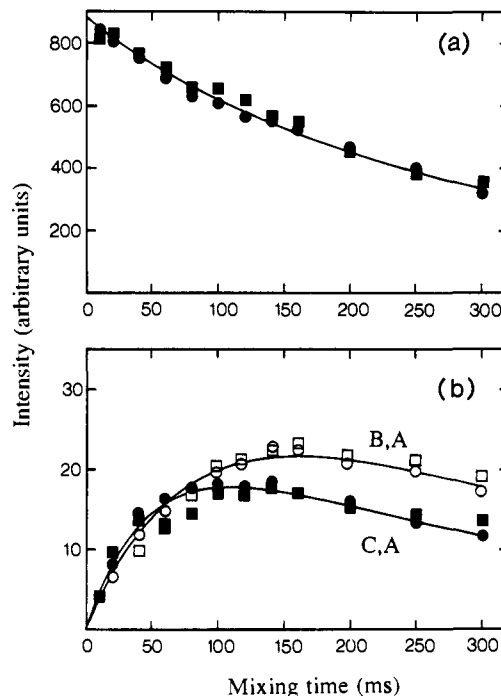


Figure 2. Comparison of the experimental and best fit calculated time dependences of (a) the diagonal resonances of the major species and (b) the exchange cross peaks between the major and minor species for the C<sup>1</sup>H protons of His-21 and His-27 in a series of NOESY spectra with mixing times ranging from 10 to 300 ms. The experimental data (at pH 5.8, 6 °C) for His-21 and His-27 are shown as circles and squares, respectively, while the lines represent the best fits obtained by integration of the differential equations given by eq 1. All the data were fitted simultaneously by using the program FACSIMILE.<sup>6</sup>

unambiguously. Because the population of species B and C is so small, no exchange cross peaks between B and C are observed as their expected intensity is below the limit of detection.

(1) Omichinski, J. G.; Clore, G. M.; Appella, E.; Sakaguchi, K.; Gronenborn, A. M. *Biochemistry* 1990, 29, 9324.

(2) (a) Davis, D. G.; Bax, A. *J. Am. Chem. Soc.* 1985, 107, 2821. (b) Bax, A. *Methods Enzymol.* 1989, 176, 151.

(3) (a) Jeener, J.; Meier, B. H.; Bachmann, P.; Ernst, R. R. *J. Chem. Phys.* 1979, 71, 4546. (b) Macura, S.; Huang, Y.; Suter, D.; Ernst, R. R. *J. Magn. Reson.* 1981, 43, 259.

(4) (a) Bothner-By, A. A.; Stephens, R. L.; Lee, J. T.; Warren, C. D.; Jeanloz, R. W. *J. Am. Chem. Soc.* 1984, 106, 811. (b) Bax, A.; Davis, D. G. *J. Magn. Reson.* 1985, 63, 207.

(5) McConnell, H. M. *J. Chem. Phys.* 1958, 28, 430.

(6) (a) Chance, E. M.; Curtis, A. R.; Jones, I. P.; Kirby, C. R. *U.K. At. Energy Auth., Harwell Lab.* 1979, AERE-R 8775. (b) Curtis, A. R. *U.K. At. Energy Auth., Harwell Lab.* 1979, AERE-R 9352. (c) Clore, G. M. In *Computing in Biological Science*; Geisow, M. J., Barrett, M., Eds.; Elsevier North-Holland: Amsterdam, 1983; p 313.